

Tuning Guidelines of a Dynamic Matrix Controller for Integrating (Non-Self-Regulating) Processes

Danielle Dougherty and Douglas J. Cooper*

Chemical Engineering Department, University of Connecticut, Storrs, Connecticut 06269-3222

Designing a multivariable dynamic matrix controller (DMC) controller for integrating processes is challenging because of the number of tuning parameters that affect the closed-loop performance. These tuning parameters required to implement DMC include the sample time; the prediction, model, and control horizons; the controlled variable weights; and the move suppression coefficients. The move suppression coefficients are used as the key tuning parameters to obtain a desirable DMC performance. This paper derives and demonstrates expressions for computing the complete set of tuning parameters for integrating processes. A novel contribution of this work is the derivation of an analytical expression for computing the move suppression coefficients based on the process model and the other DMC design parameters. The tuning rules are demonstrated on simulated processes including a constrained multivariable process simulation that displays integrating characteristics.

1. Introduction

Designing a DMC controller for integrating (non-self-regulating) processes is challenging because of the number of adjustable parameters that affect the closed-loop performance. The parameters required to implement DMC include the sample time; the prediction, model, and control horizons; the controlled variable weights; and the move suppression coefficients. This work presents expressions for computing the complete set of tuning parameters for processes that display integrating behavior. Perhaps the largest contribution of this work is the derivation of a novel analytical expression for computing the move suppression coefficients based on the model and other DMC design parameters.

The move suppression coefficients are used as the primary tuning parameters to obtain desirable DMC performance. They serve a dual purpose in the DMC control law. Their primary role in DMC is to suppress aggressive control actions. Additionally, they are used to improve the conditioning of the system matrix.

The derivation of the move suppression coefficients exploits the correlation between the condition numbers of the partitioned blocks in the system matrix and the controller output move sizes. The move suppression coefficients, which modify the condition numbers of the block partitions of the system matrix, are computed such that the condition numbers are always bounded by a fixed low value. When the condition numbers are constrained at a low value, a desirable DMC closed-loop performance is achieved.

The illustrative applications presented show that the design technique is able to produce a consistent closed-loop performance for systems displaying integrating characteristics. The tuning strategy is validated for set-point tracking performance and disturbance rejection.

2. Background

2.1. DMC Control Law. The multivariable DMC controller has been discussed extensively by past researchers^{1–3} and is summarized here for the convenience of the reader. For a system with S controller outputs and R measured process variables, the multivariable DMC quadratic performance objective function has the form⁴

$$\text{Min}_{\Delta \bar{\mathbf{u}}} J = [\bar{\mathbf{e}} - \mathbf{A}\Delta \bar{\mathbf{u}}]^T \mathbf{\Gamma}^T \mathbf{\Gamma} [\bar{\mathbf{e}} - \mathbf{A}\Delta \bar{\mathbf{u}}] + [\Delta \bar{\mathbf{u}}]^T \mathbf{\Lambda}^T \mathbf{\Lambda} [\Delta \bar{\mathbf{u}}] \quad (1)$$

subject to:

$$\hat{y}_{r,\min} \leq \hat{y}_r \leq \hat{y}_{r,\max} \quad (2)$$

$$\Delta \bar{\mathbf{u}}_{s,\min} \leq \Delta \bar{\mathbf{u}}_s \leq \Delta \bar{\mathbf{u}}_{s,\max} \quad (3)$$

$$\bar{\mathbf{u}}_{s,\min} \leq \bar{\mathbf{u}}_s \leq \bar{\mathbf{u}}_{s,\max} \quad (4)$$

A closed-form solution to the multivariable DMC performance objective results in the unconstrained multivariable DMC control law:⁴

$$\Delta \bar{\mathbf{u}} = (\mathbf{A}^T \mathbf{\Gamma}^T \mathbf{\Gamma} \mathbf{A} + \mathbf{\Lambda}^T \mathbf{\Lambda})^{-1} \mathbf{A}^T \mathbf{\Gamma}^T \mathbf{\Gamma} \bar{\mathbf{e}} \quad (5)$$

Here, \mathbf{A} is the multivariable dynamic matrix formed from the unit step response coefficients of each controller output to measured process variable pair. $\bar{\mathbf{e}}$ is the vector of predicted errors for the R measured process variables over the next P sampling instants (prediction horizon). $\Delta \bar{\mathbf{u}}$ is the vector of controller output changes for the S controller output variables computed for the next M sampling instants (control horizon). \hat{y}_r is the predicted process variable profile for the r th measured process variable over the next P sampling instances. $\mathbf{\Gamma}^T \mathbf{\Gamma}$ is the matrix of controlled variable weights and $\mathbf{\Lambda}^T \mathbf{\Lambda}$ is the matrix of move suppression coefficients.

$\mathbf{\Lambda}^T \mathbf{\Lambda}$ is a square-diagonal matrix of dimensions $M \cdot S \times M \cdot S$. The leading diagonal elements of the i th $M \times M$ matrix block along the diagonal of $\mathbf{\Lambda}^T \mathbf{\Lambda}$ are λ_i^2 . All off-diagonal elements are zero. Hence, in the multivariable DMC control law (eq 5), the move suppression

* To whom correspondence should be addressed. Tel.: (860) 486-4092. Fax: (860) 486-2959. E-mail: cooper@enr.uconn.edu.

Table 1. Tuning Guidelines for DMC of Self-Regulating Processes

1. approximate the process dynamics of all controller output to measured process variable pairs with FOPDT models

$$\tau_{p_{rs}} \frac{dy_r(t)}{dt} + y_r(t) = K_{p_{rs}} u_s(t - \theta_{p_{rs}}) \quad \text{or} \quad \frac{y_r(s)}{u_s(s)} = \frac{K_{p_{rs}} e^{-\theta_{p_{rs}} s}}{\tau_{p_{rs}} s + 1}$$

$$r = 1, 2, \dots, R; s = 1, 2, \dots, S$$

2. select the sample time as close as possible to

$$\begin{cases} T_{rs} = \text{Max}(0.1\tau_{p_{rs}}, 0.5\theta_{p_{rs}}) \\ T = \text{Min}(T_{rs}) \end{cases} \quad (r = 1, 2, \dots, R; s = 1, 2, \dots, S)$$

3. compute the prediction horizon, P , and the model horizon, N

$$P = N = \text{Max} \left[\text{Int} \left(\frac{5\tau_{p_{rs}}}{T} \right) + k_{rs} \right] \quad \text{where } k_{rs} = \text{Int} \left(\frac{\theta_{p_{rs}}}{T} \right) + 1$$

$$r = 1, 2, \dots, R; s = 1, 2, \dots, S$$

4. compute a control horizon, M

$$M = \text{Max} \left[\text{Int} \left(\frac{\tau_{p_{rs}}}{T} \right) + k_{rs} \right] \quad (r = 1, 2, \dots, R; s = 1, 2, \dots, S)$$

5. select the controlled variable weights, γ_r^2 , to scale process variable units to be the same

6. compute the move suppression coefficients, λ_s^2

$$\lambda_s^2 = \frac{M}{10} \sum_{r=1}^R \left[\gamma_r^2 K_{p_{rs}}^2 \left\{ P - k_{rs} - \frac{3\tau_{p_{rs}}}{2T} + 2 - \frac{M-1}{2} \right\} \right] \quad (s = 1, 2, \dots, S)$$

or

$$\lambda = \frac{M}{10} \left\{ \frac{3.5\tau_p}{T} + 2 - \frac{M-1}{2} \right\} K_p^2 \quad (\text{for } s = 1, \text{ single-loop DMC})$$

7. implement DMC using the traditional step response matrix of the actual process and the initial values of the parameters computed in steps 1–6

coefficients that are added to the leading diagonal of the system matrix ($\mathbf{A}^T \mathbf{\Gamma}^T \mathbf{\Gamma} \mathbf{A}$) are λ_i^2 ($i = 1, 2, \dots, S$). Similarly, the $P \cdot R \times P \cdot R$ matrix of controlled variable weights, $\mathbf{\Gamma}^T \mathbf{\Gamma}$, has the leading diagonal elements as γ_i^2 ($i = 1, 2, \dots, R$). Again, all off-diagonal elements are zero.

2.2. Summary of Tuning Rules for Self-Regulating Processes. The tuning rules for DMC^{5,6} are based on fitting the controller output to measured process variable dynamics for each subprocess relating the s th controller output to the r th process variable at the design level of operation with a FOPDT model approximation. Table 1 displays the guidelines for determining the DMC tuning parameters for self-regulating processes.

3. Challenge of Integrating Processes

A base case process is employed to illustrate the performance of DMC for a step change in the set-point of an integrating process:

$$G_p(s) = \frac{y(s)}{u(s)} = \frac{0.01e^{-10s}}{s(100s + 1)} \quad (6)$$

The process given in eq 6 is used to show the poor performance of DMC when tuned using the self-regulating process rules summarized in Table 1. Based on the minimum sum of squared errors, a FOPDT model approximation of the process given in eq 6 yields a process gain, $K_p = 27$, an overall time constant, $\tau_p = 3960$, and an effective dead time, $\theta_p = 2.5$. The sample time calculated for this process using the equation given in Table 1 is $T = 100$. Continuing with the tuning guidelines given in Table 1, $P = N = 198$, $M = 40$, and $\lambda = 3.53 \times 10^5$.

Figure 1 displays a graph of the process variables' response using the DMC algorithm and the tuning

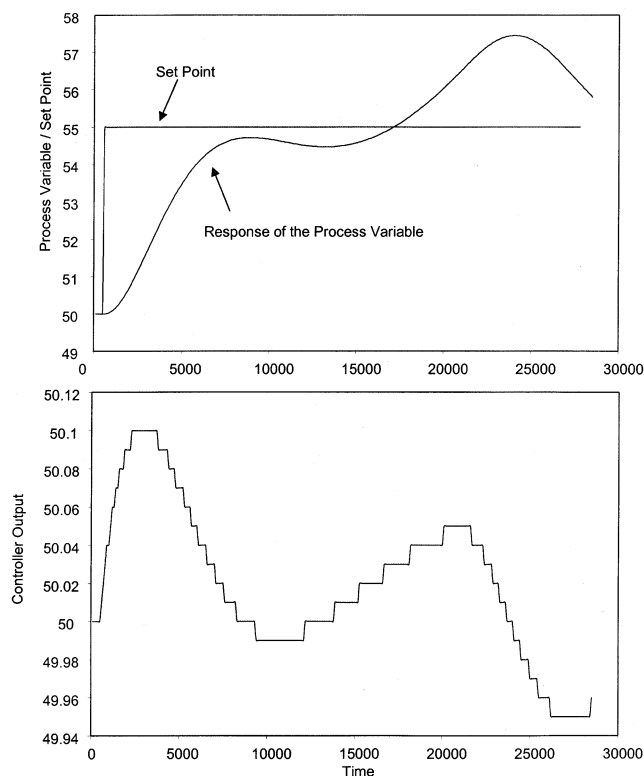


Figure 1. Performance of DMC for integrating processes using the original DMC algorithm and the existing tuning guidelines ($T = 100$, $P = N = 198$, $M = 40$, and $\lambda = 3.53 \times 10^5$).

parameters given above. The poor performance is evident in this set-point tracking example because the response of the process variable has a very long rise time and eventually the process becomes unstable.

3.1. Modification of the DMC Algorithm. One of the limitations of DMC is that it requires the internal

DMC step response process model to describe a stable plant.^{4,7} The predicted process variable profile, $\hat{y}(n+j)$, over j sampling instants ahead of the current time, n , is calculated as

$$\hat{y}(n+j) = y_0 + \underbrace{\sum_{i=1}^j a_i \Delta u(n+j-i)}_{\text{Effect of current and future moves}} + \underbrace{\sum_{i=j+1}^{N-1} a_i \Delta u(n+j-i)}_{\text{Effect of past moves}} \quad (7)$$

where a_i is the i th unit step response coefficient of the process. Because the current and future controller output moves have not been determined, eq 7 reduces to

$$\hat{y}(n+j) = y_0 + \sum_{i=j+1}^{N-1} a_i \Delta u(n+j-i) + d(n+j) \quad (8)$$

where the term $d(n+j)$ is the disturbance estimate. The current and future values of the disturbance estimate are calculated as

$$d(n+j) = d(n) = y(n) - y_0 - \sum_{i=1}^{N-1} a_i \Delta u(n-i) \quad (9)$$

where $y(n)$ is the current process variable measurement.

In the formulation given above, the step response coefficient at the N th sample into the future is assumed to be approximately equal the step response coefficient at steady state. For integrating processes, the N th step response coefficient does not equal the step response coefficient at steady state. Thus, these equations can no longer be employed.

There has been little research performed focusing on extending DMC to handle integrating processes. Some researchers^{7,8} have presented state-space-based MPC algorithms that are able to handle integrating processes. Another method is to modify the computation used to predict the process variable profile.⁹ In this case, the DMC algorithm does not need to be recast into the state-space form and the remainder of the control calculations remain the same, which makes it simpler to implement.

Specifically, Gupta⁹ takes advantage of the process dynamics of an integrating process. The modified formulation of DMC for integrating processes uses the fact that the measured process variable response due to the past controller output moves is just a straight line passing through the current measurement of the process variable at the current control instant. Hence, the predicted process variable profile is calculated as a slope projection.

The modified DMC algorithm⁹ calculates the predicted process variable profile, $\hat{y}(n+j)$ as

$$\hat{y}(n+j) = y_0 + j[y(n) - y(n-1)] \quad (j = 1, 2, \dots, N) \quad (10)$$

where $y(n)$ is the process variable measurement at the current control instant and $y(n-1)$ is the process vari-

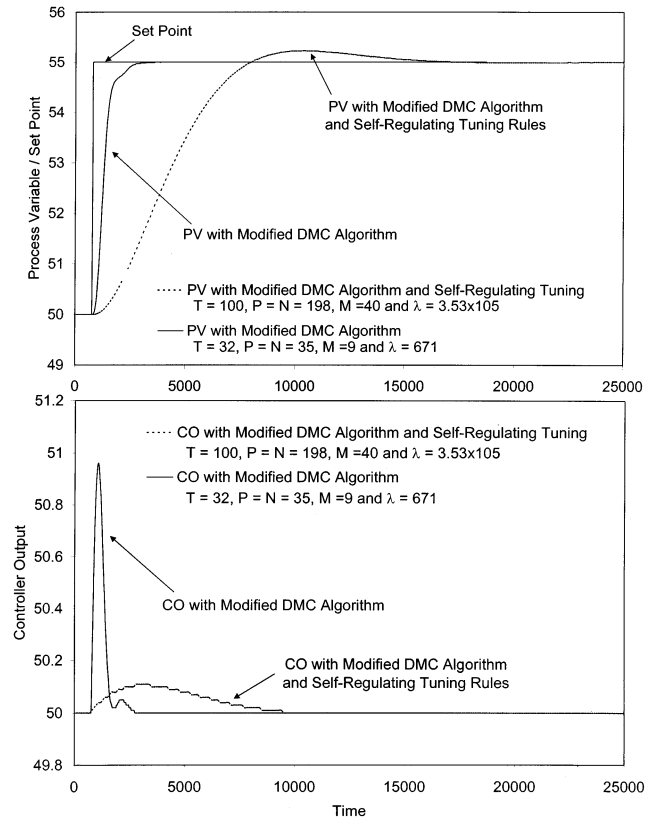


Figure 2. Importance of the tuning parameters on the performance of DMC for integrating processes ($T = 32$, $P = N = 35$, $M = 9$, and $\lambda = 671$; $T = 100$, $P = N = 198$, $M = 40$, and $\lambda = 3.53 \times 10^5$).

able measurement at the previous control instant. Similarly, the disturbance estimate, $d(n+j)$, is modified as

$$d(n+j) = d(n) = y(n) - y_0 - [y(n) - y(n-1)] \quad (11)$$

To extend this to multivariable problems in which some of the subprocesses exhibiting integrating characteristics are straightforward, the predicted process variable profile and disturbance estimate for all open-loop stable subprocesses are calculated in the usual method using eqs 7–9. Only the subprocesses that exhibit integrating behavior use eqs 10 and 11 to calculate the predicted process variable profile and the disturbance estimate.

The base case given in eq 6 is employed to illustrate the importance of the tuning parameters on the response of DMC for a step change in the set-point. Figure 2 displays the process variable response using the modified DMC algorithm (eqs 7–9), and the tuning rules for the self-regulating process are summarized in Table 1. Using the guidelines given in Table 1, $T = 100$, $P = N = 198$, $M = 40$, and $\lambda = 3.53 \times 10^5$. The graph also shows the performance of the modified DMC algorithm when other tuning parameters (such as those given in eqs 12–17 and 44) are employed. For this case, $T = 32$, $P = N = 35$, $M = 9$, and $\lambda = 671$.

The control objective is the set-point tracking performance of the DMC controller. The design goal is a fast rise time with no peak overshoot ratio.

Figure 2 shows the response of the process variable for both the original and modified DMC implementations. As illustrated by the figure, both sets of tuning

guidelines are able to give stable responses; however, the rise time is much longer for the response tuned using the self-regulating tuning guidelines, and the response has about a 5% peak overshoot ratio. The rise time is approximately 7200 s for this response. The rise time for the DMC tuned using eqs 12–17 and 44 is only 2200 s. Hence, the tuning guidelines for the DMC of integrating processes need to be derived based on an integrating model approximation of the process in order to achieve a fast rise time with no peak overshoot ratio.

3.2. Derivation of the DMC Tuning Rules. Because of the unusual dynamics of an integrating process, a FOPDT integrating model approximation should be employed. A FOPDT integrating model approximation has the form

$$\frac{dy(t)}{dt} = K_p^* u(t - \theta_p) \quad \text{or} \quad \frac{y(s)}{u(s)} = \frac{K_p^* e^{-\theta_p s}}{s} \quad (12)$$

where K_p^* is the integrator gain and θ_p is the effective dead time. Past researchers^{10,11} have used a FOPDT integrating model for tuning PI and PID controllers. It is emphasized here that the use of this FOPDT integrating model approximation is employed only in the derivation of the tuning parameters used in DMC. The examples presented later in this work all use the traditional dynamic matrix and the predicted process variable profile calculated using the actual process data upon implementation.

Using the FOPDT integrating model parameters, the sample time, T , is computed such that the process is sampled two to three times per effective dead time¹² or

$$T \leq 0.5\theta_p \quad (13)$$

Hence, this value of sample time balances the desire for a low computation load (a large T) with the need to properly track the dynamic behavior of an integrating process (a small T). Recognizing that many control computers restrict the choice of T ,^{13,14} the remaining tuning rules permit values of T other than that computed by eq 13 to be used.

The discrete dead time is calculated in integer samples as

$$k = \text{Int}(\theta_p/T) + 1 \quad (14)$$

The remaining tuning parameters are related directly to the closed-loop speed of the response and the robustness of the control loop. Hence, the tuning guidelines are based on the closed-loop time constant of the system. In general, a small closed-loop time constant corresponds to a faster closed-loop response with large variations in the controller output. A large closed-loop time constant displays a slower and smoother response.

Tyres and Luyben¹¹ showed that the closed-loop time constant for a FOPDT integrating model can be approximated as

$$\tau_{CL} = \theta_p \sqrt{10} \quad (15)$$

The prediction horizon, P , and the model horizon, N , are computed as the closed-loop process settling time in samples as

$$P = N = \text{Int}(5\tau_{CL}/T) + k \quad (16)$$

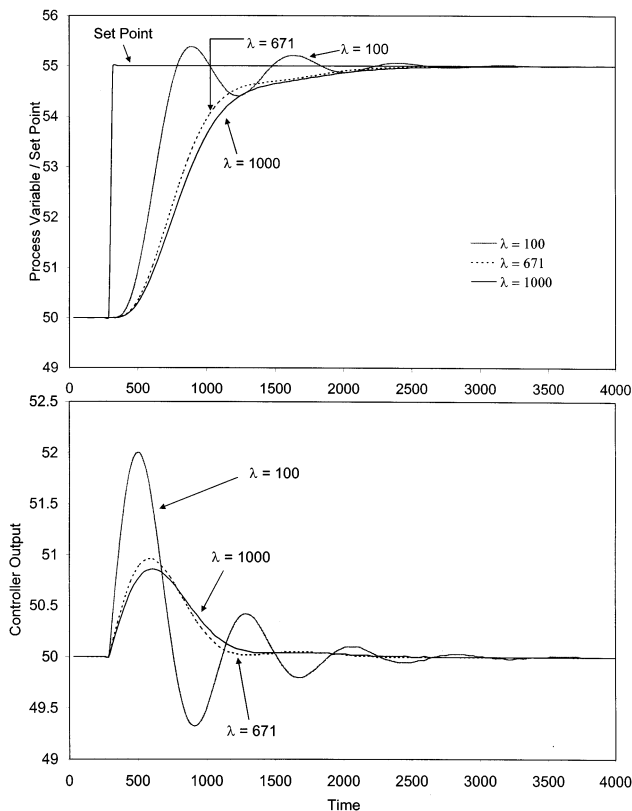


Figure 3. Importance of the move suppression coefficient, λ , in tuning the modified DMC algorithm ($T = 32$, $P = N = 35$, and $M = 9$).

Note that both N and P cannot be selected independently of the sample time.

A larger P improves the nominal stability of the closed-loop. For this reason, P is selected such that it includes the steady-state effect of all past controller output moves; i.e., it is calculated as the closed-loop settling time of the FOPDT integrating model approximation.

In addition, it is important that N be equal to the closed-loop settling time of the process to avoid truncation error in the predicted process variable profile. Hence, eq 16 computes N as the closed-loop settling time of the FOPDT integrating model approximation. This value is long enough to avoid the instabilities that can otherwise result because truncation of the model horizon misrepresents the effect of past controller output moves in the predicted process variable profile.⁷

In the examples that follow, eq 16 gives values for P and N ranging between 30 and 40. These values are in line with observations of past researchers. For example, Prett and Garcia¹⁵ and Maurath and co-workers¹⁶ have shown that the values calculated for P and N should range between 20 and 70. Also, the value typically selected in industry is approximately 30.^{1,7}

The control horizon, M , must be long enough such that the results of the control actions are clearly evident in the response of the measured process variable. The tuning rule thus chooses M as

$$M = \text{Int}(\tau_{CL}/T) + k \quad (17)$$

Figure 3 illustrates the importance of λ in tuning the modified DMC algorithm. A FOPDT integrating model approximation of the process described in eq 12 yields

an integrator gain, $K_p^* = 0.008$, and an effective dead time, $\theta_p = 65$. The closed-loop time constant, τ_{CL} , calculated using eq 15 is 205. The value of the sample time, T , calculated using eq 13 is 32. Using eq 16, the prediction horizon, P , and model horizon, N , are equal to 35. The value of the control horizon, M , calculated using eq 17 is 9.

The control objective is the set-point tracking performance capabilities of DMC due to a step change in the set-point. A desirable closed-loop performance is defined as a fast rise time with no peak overshoot ratio.

Figure 3 shows the impact of λ on the response of the process variable for the modified DMC algorithm and the value of the tuning parameters given above. For a value of λ equal to 100, the process variable response exhibits a large peak overshoot ratio and a long settling time. For a value of λ equal to 671, the response displays no overshoot and a rise time of 2800 s. For a value of λ equal to 1000, the response shows that a larger move suppression coefficient results in a slower response. Further increasing λ leads to an undesirable sluggish response for most applications. Thus, this study shows that the choice of λ is critical to the performance achieved by DMC.

3.3. Derivation of the Move Suppression Coefficient. The final step in the design of the DMC controller is the calculation of the move suppression coefficient, λ . Past researchers³ have indicated that the move suppression coefficient, λ , suppresses aggressive controller action when $M > 1$ and improves the conditioning of the system matrix by rendering it more positive definite.

Previous work has shown that the choice of the move suppression coefficient for DMC can be made independently of the process gain.^{5,6} Gain scaling is a term to represent a modification where a mathematical expression is stripped of the effects of the process gain for analysis independent of the gain.

For integrating processes, the move suppression coefficient must be gain- and time-scaled because the units for the process gain are

$$K_p^* [=] \frac{y(t)}{u(t) \cdot t} \quad (18)$$

Hence, the move suppression coefficient is expressed as a product of the scaled move suppression coefficient, f , and the square of the process gain and sample time, $[K_p^* T]^2$.

Consider the move suppression coefficient written as

$$\lambda = f [K_p^* T]^2 \quad (19)$$

The step response coefficients of any linear integrating system can be written as

$$a_j = K_p^* T \tilde{a}_j \quad (20)$$

where \tilde{a}_j represents the part of the unit step response coefficient that is independent of the process gain, K_p^* , and the sample time, T . By using eqs 19 and 20, the

gain and time effects can be separate from the first row elements, c_i , of the pseudo inverse matrix:

$$\begin{aligned} c_i &= i\text{th first-row element of } \{(\mathbf{A}^T \mathbf{A} + \lambda \mathbf{I})^{-1} \mathbf{A}^T\} \\ &= i\text{th first-row element of} \\ &\quad \{[(K_p T)^2 \tilde{\mathbf{A}}^T \tilde{\mathbf{A}} + f(K_p T)^2 \mathbf{I}]^{-1} K_p^* \tilde{\mathbf{A}}^T\} \\ &= \frac{1}{K_p^* T} \times i\text{th first-row element of} \\ &\quad \{(\tilde{\mathbf{A}}^T \tilde{\mathbf{A}} + f \mathbf{I})^{-1} \tilde{\mathbf{A}}^T\} \\ &= \frac{\tilde{c}_i}{K_p^* T} \end{aligned} \quad (21)$$

Here, $\tilde{\mathbf{A}}$ is the gain- and time-scaled dynamic matrix, $\tilde{\mathbf{A}}^T \tilde{\mathbf{A}}$ is the gain- and time-scaled system matrix, and \tilde{c}_i is the i th first-row element of the gain- and time-scaled pseudo inverse matrix.

The development of the DMC transfer function is given in the literature^{5,6,17,18} in the z domain as

$$D(z) = \frac{u(z)}{e(z)} = \frac{1}{(1 - z^{-1}) \left[\frac{1}{\sum_{i=1}^P c_i} + \sum_{j=1}^{N-1} \left(\frac{\sum_{i=1}^P c_i a_{i+j}}{\sum_{i=1}^P c_i} - a_j \right) z^{-j} \right]} \quad (22)$$

Substituting eqs 20 and 21 into eq 22 shows that the gain and time dependence of the single-loop DMC transfer function is separable from the dependence on the remaining process and controller parameters:

$$D(z) = \frac{u(z)}{e(z)} = \frac{1}{K_p^* T \left[\frac{1}{\sum_{i=1}^P \tilde{c}_i} + \sum_{j=1}^{N-1} \left(\frac{\sum_{i=1}^P \tilde{c}_i \tilde{a}_{i+j}}{\sum_{i=1}^P \tilde{c}_i} - \tilde{a}_j \right) z^{-j} \right]} = \frac{\tilde{D}(z)}{K_p^* T} \quad (23)$$

Similarly, the gain and time dependence of a linear integrating process transfer function is separable from the remaining process parameters:

$$G(z) = \frac{y(z)}{u(z)} = K_p^* T \tilde{G}(z) \quad (24)$$

Using eqs 23 and 24, the open-loop transfer function has the form

$$D(z) G(z) = \frac{y(z)}{e(z)} = \frac{\tilde{D}(z)}{K_p^* T} K_p^* T \tilde{G}(z) = \tilde{D}(z) \tilde{G}(z) \quad (25)$$

and the closed-loop transfer function has the form

$$\frac{y(z)}{y_{sp}(z)} = \frac{D(z) G(z)}{1 + D(z) G(z)} = \frac{\tilde{D}(z) \tilde{G}(z)}{1 + \tilde{D}(z) \tilde{G}(z)} \quad (26)$$

When the move suppression coefficient, λ , is expressed as a scaled coefficient, f , times the square of the process gain and sample time, $[K_p^* T]^2$, the closed-loop performance is independent of the process gain and sample time. As a result, the derivation of an analytical expression for λ yields a scaled coefficient, f , as a function of parameters other than the process gain and sample time.

The derivation of the analytical expression for λ is made possible by using a FOPDT integrating model approximation of the process. A FOPDT integrating model with zero-order hold is represented by a discrete transfer function as

$$H_0 G_p(z) = \frac{K_p^* T z^{-k}}{1 - z^{-1}} \quad (27)$$

where K_p^* is the integrator gain, T is the discrete sample time, and k is the effective discrete dead time given by eq 14.

From eq 27, the gain- and time-scaled step response coefficients of a FOPDT integrating process are given by

$$\tilde{a}_i = \begin{cases} 0 & 0 \leq j \leq k - 1 \\ j - k + 1 & k \leq j \end{cases} \quad (28)$$

Using a FOPDT integrating model approximation of the process and the gain- and time-scaled step response coefficients from eq 28, the dynamic matrix has the form

$$\tilde{\mathbf{A}} = \begin{bmatrix} \tilde{a}_1 & 0 & 0 & \cdots & 0 \\ \tilde{a}_2 & \tilde{a}_1 & 0 & & 0 \\ \tilde{a}_3 & \tilde{a}_2 & \tilde{a}_1 & \cdots & 0 \\ \vdots & \vdots & \vdots & & 0 \\ \tilde{a}_M & \tilde{a}_{M-1} & \tilde{a}_{M-2} & & \tilde{a}_1 \\ \vdots & \vdots & \vdots & & \vdots \\ \tilde{a}_P & \tilde{a}_{P-1} & \tilde{a}_{P-2} & \cdots & \tilde{a}_{P-M+1} \end{bmatrix}_{P \times M} \Rightarrow \tilde{\mathbf{A}} = \begin{bmatrix} 0 & 0 & 0 & \cdots & 0 \\ \vdots & \vdots & \vdots & & \vdots \\ 0 & 0 & 0 & \cdots & 0 \\ 1 & 0 & 0 & \cdots & 0 \\ 2 & 1 & 0 & \cdots & 0 \\ 3 & 2 & 1 & \cdots & 0 \\ \vdots & \vdots & \vdots & & 0 \\ M & M-1 & M-2 & \cdots & 1 \\ \vdots & \vdots & \vdots & & \vdots \\ P-k+1 & P-k & P-k-1 & \cdots & P-k-M+1 \end{bmatrix}_{P \times M} \quad (29)$$

Based on the dynamic matrix given above, the gain- and time-scaled system matrix, $\tilde{\mathbf{A}}^T \tilde{\mathbf{A}}$, in the DMC control

law has the form

$$\tilde{\mathbf{A}}^T \tilde{\mathbf{A}} = \begin{bmatrix} \sum_{i=1}^{P-k+1} i^2 & \sum_{i=2}^{P-k+1} i(i-1) & \sum_{i=3}^{P-k+1} i(i-2) & \cdots \\ \sum_{i=2}^{P-k+1} i(i-1) & \sum_{i=2}^{P-k+1} (i-1)^2 & \sum_{i=3}^{P-k+1} (i-1)(i-2) & \cdots \\ \sum_{i=3}^{P-k+1} i(i-2) & \sum_{i=3}^{P-k+1} (i-1)(i-2) & \sum_{i=3}^{P-k+1} (i-2)^2 & \cdots \\ \vdots & \vdots & \vdots & \cdots \end{bmatrix}_{M \times M} \quad (30)$$

An approximate form of the gain- and time-scaled system matrix can be obtained by approximating the individual terms of the matrix in eq 30 for large values of the prediction horizon, P . Let $\tilde{\alpha}_{ij}$ ($i, j = 1, 2, \dots, M$) be the term in the i th row and j th column of the gain- and time-scaled system matrix. The approximation of one such term, $\tilde{\alpha}_{11}$, is shown in eq 31.

Recognizing that the summation terms in $\tilde{\alpha}_{11}$ are in a geometric progression results in the exact expression

$$\tilde{\alpha}_{11} = \sum_{i=1}^{P-k+1} i^2 = \frac{(P-k+1)^3}{3} + \frac{(P-k+1)^2}{2} + \frac{P-k+1}{6} \quad (31)$$

With a FOPDT integrating model approximation available, the prediction horizon, P , can be computed as the closed-loop process settling time in samples as $P = \text{Int}(5\tau_{CL}/T) + k$. Past researchers^{4,7,16} have found that P should be large enough to include the steady-state effect of all past controller output moves.

For large values of the prediction horizon, eq 31 simplifies to

$$\tilde{\alpha}_{11} \cong \frac{(P-k+1)^3}{3} \quad (32)$$

As P increases, the approximation in eq 32 becomes increasingly accurate. The other terms of the $\tilde{\mathbf{A}}^T \tilde{\mathbf{A}}$ matrix can be approximated in a similar fashion. Let $n = P - k + 1$ and $\beta = \tilde{\alpha}_{11} \cong n^3/3$; then the final approximate form of the matrix that results is

$$\tilde{\mathbf{A}}^T \tilde{\mathbf{A}} = \begin{bmatrix} \beta & \beta & \beta - \frac{n^2}{2} & \cdots \\ \beta & \beta - \frac{n^2}{2} & \beta - n^2 & \cdots \\ \beta - \frac{n^2}{2} & \beta - n^2 & \beta - \frac{3n^2}{2} & \cdots \\ \vdots & \vdots & \vdots & \cdots \end{bmatrix}_{M \times M} \quad (33)$$

Now, the $\tilde{\mathbf{A}}^T \tilde{\mathbf{A}} + f\mathbf{I}$ matrix, to be inverted in the

DMC control law, has the form

$$\tilde{\mathbf{A}}^T \tilde{\mathbf{A}} + f \mathbf{I} = \begin{bmatrix} \beta + f & \beta & \beta - \frac{n^2}{2} & \cdots \\ \beta & \beta - \frac{n^2}{2} + f & \beta - n^2 & \cdots \\ \beta - \frac{n^2}{2} & \beta - n^2 & \beta - \frac{3n^2}{2} + f & \cdots \\ \vdots & \vdots & \vdots & \cdots \end{bmatrix}_{M \times M} \quad (34)$$

Equation 34 can be used to determine explicitly analytical expressions for the eigenvalues of $\tilde{\mathbf{A}}^T \tilde{\mathbf{A}} + f \mathbf{I}$.

The minimum eigenvalue of $\tilde{\mathbf{A}}^T \tilde{\mathbf{A}} + f \mathbf{I}$ is determined by noting that the $\tilde{\mathbf{A}}^T \tilde{\mathbf{A}}$ matrix (eq 33) is nearly singular for $M = 2$ and is perfectly singular for $M > 2$. Therefore, the minimum absolute eigenvalue of $\tilde{\mathbf{A}}^T \tilde{\mathbf{A}}$ for $M \geq 2$ is close to or exactly zero. When a constant quantity, f , is added to the leading diagonal of such a matrix, all of its eigenvalues are shifted by that quantity.^{3,19} Hence, the minimum absolute eigenvalue of the resultant $\tilde{\mathbf{A}}^T \tilde{\mathbf{A}} + f \mathbf{I}$ matrix, μ_{\min} , is equal to f or

$$\mu_{\min} = f \quad (35)$$

Analytical expressions for the maximum eigenvalue can be derived for the square matrix, $\tilde{\mathbf{A}}^T \tilde{\mathbf{A}} + f \mathbf{I}$, with consecutively increases in the dimensions $M \times M$. A general formula for the maximum eigenvalue can be obtained as a function of M by recognizing that the coefficients follow a pattern that is a function of the matrix dimension $M \times M$.

For M equal to 2, the analytical expression for the maximum eigenvalue can be approximated for large values of P as

$$\mu_{\max} = \frac{1}{2}(2\beta + 2f - 0.5n^2 + 2\sqrt{\beta^2 + 0.0625n^4}) \cong \frac{1}{2}(2\beta + 2f - 0.5n^2 + 2\beta) \quad (\text{for large } P) \quad (36)$$

Equations for the maximum eigenvalue for M equal to 3–5 can also be determined. For large values of P , the expressions for the maximum eigenvalue for M equal to 3–5 can be approximated as

$$\begin{aligned} \mu_{\max} &\cong \frac{1}{3}(3\beta + 3f - 2n^2 + 6\beta) && \text{for } M=3 \\ \mu_{\max} &\cong \frac{1}{4}(4\beta + 4f - 4.5n^2 + 12\beta) && \text{for } M=4 \\ \mu_{\max} &\cong \frac{1}{5}(5\beta + 5f - 8n^2 + 20\beta) && \text{for } M=5 \end{aligned} \quad (37)$$

By comparison of the equation for the maximum eigenvalue for M equal to 2–5 (eqs 36 and 37), a general analytical expression for the maximum eigenvalue can be obtained. The general expression has the form

$$\mu_{\max} \cong \frac{1}{w}(v\beta + qf - bn^2) \quad (38)$$

The coefficients w , v , and q are found by comparing eq 36 to eq 38. The coefficient that multiplies the entire

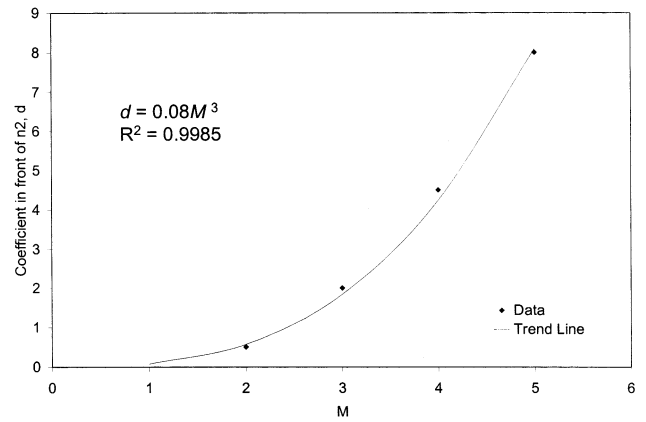


Figure 4. Nonlinear regression for d in eq 38.

equation is just 1 divided by w , where w is equal to M . The coefficient in front of β is equal to M^2 . The coefficient in front of f , q , is found to be equal to M .

The coefficient in front of n^2 is determined by nonlinear regression. Figure 4 shows a plot of M versus the coefficient in front of n^2 and the nonlinear regression. As shown by the graph, the coefficient in front of n^2 can be expressed as

$$\text{coefficient in front of } n^2 = b \cong 0.08M^3 \quad (39)$$

From this, the general analytical expression for the maximum eigenvalue is given as

$$\mu_{\max} \cong \frac{1}{M}(M^2\beta + Mf - 0.08M^3n^2) \quad (40)$$

Past researchers³ have shown that the move suppression coefficient, λ , serves two purposes in the DMC control law. Its primary role in DMC is to suppress aggressive controller actions when $M > 1$. In addition, λ improves the conditioning of the system matrix by making it more positive definite.

For example, when λ is increased, the controller output move sizes and the condition number decrease. When an analytical expression is determined for the effect of λ on the condition number of the system matrix, the condition number can be maintained within specified bounds by an appropriate choice for λ . Hence, an upper bound on the condition number would, prevent the controller output move sizes from becoming too large.

The condition number for a square matrix is defined as

$$c = |\mu_{\max}|/|\mu_{\min}| \quad (41)$$

From eqs 35, 40, and 41, the condition number for the $\tilde{\mathbf{A}}^T \tilde{\mathbf{A}} + f \mathbf{I}$ matrix is

$$c = \frac{1}{Mf}(M^2\beta + Mf - 0.08M^3n^2) \quad (42)$$

Equation 42 is rearranged to give an expression for the scaled move suppression coefficient as

$$f = \frac{1}{cM}(M^2\beta - 0.08M^3n^2) \quad (43)$$

where $\beta = n^3/3$ and $n = P - k + 1$.

Past researchers^{5,6} have indicated a typical condition number of 10. Following this, a condition number of 10

Table 2. Tuning Guidelines for SISO DMC of Integrating (Non-Self-Regulating) Processes

1. approximate the process dynamics of the controller output to measured process variable pair with the FOPDT integrating model

$$\frac{dy(t)}{dt} = K_p^* u(t - \theta_p) \quad \text{or} \quad \frac{y(s)}{u(s)} = \frac{K_p^* e^{-\theta_p s}}{s}$$

2. select the sample time as close as possible to

$$T \leq 0.5\theta_p$$

3. compute the discrete dead time

$$k = \text{Int}\left(\frac{\theta_p}{T} + 1\right)$$

4. approximate the closed-loop time constant

$$\tau_{\text{CL}} = \theta_p \sqrt{10}$$

5. compute the prediction horizon, P , and the model horizon, N

$$P = N = \text{Int}\left(\frac{5\tau_{\text{CL}}}{T}\right) + k$$

6. compute a control horizon, M

$$M = \text{Int}\left(\frac{\tau_{\text{CL}}}{T}\right) + k$$

7. compute the move suppression coefficient, λ

$$f = \frac{1}{10M} \left[\frac{M^2(P - k + 1)^3}{3} - 0.08M^3(P - k + 1)^2 \right]$$

$$\lambda = f[K_p^* T]^2$$

8. implement DMC using the traditional step response matrix of the actual process and the initial values of the parameters computed in steps 1–7

is selected to represent a modest control effort. However, the choice of the condition number lies with the individual control practitioner. If a faster or slower closed-loop response is more desirable, a larger or smaller condition number, respectively, can be used instead.

When the expressions for β and n are substituted into eq 43, the analytical expression for the move suppression coefficient, λ , is given by

$$f = \frac{1}{10M} \left[\frac{M^2(P - k + 1)^3}{3} - 0.08M^3(P - k + 1)^2 \right] \quad (44)$$

$$\lambda = f[K_p^* T]^2$$

Equation 44 is valid for a control horizon greater than 1 ($M > 1$). When the control horizon is 1 ($M = 1$), no move suppression coefficient should be used ($\lambda = 0$). The tuning guidelines for SISO DMC of integrating processes are summarized in Table 2.

4. Extension of the Tuning Strategy to Multivariable Systems

The design of a multivariable DMC is considerably more challenging for the control practitioner. The analytical expression that computes the move suppression coefficient (eq 44) developed in the previous section for single-loop DMC for integrating processes provides the foundation upon which a similar analytical expression can be developed for multivariable DMC where some of the loops display integrating behavior. This is possible in a straightforward fashion even though the performance objective for multivariable DMC is defined over several controller outputs and measured outputs and results in a more complex DMC control law.

Similar to single-loop DMC, the move suppression coefficients are employed as the primary tuning parameter for multivariable DMC in order to obtain a desired closed-loop performance. Because the dual benefit of the move suppression coefficients, λ_i^2 , is to improve

the conditioning of the multivariable DMC system matrix ($\mathbf{A}^T \mathbf{\Gamma}^T \mathbf{\Gamma} \mathbf{A}$) and suppress the controller output move sizes, a strategy similar to single-loop DMC can be used to extend eq 44 to compute the move suppression coefficients for multivariable DMC where some of the loops display integrating characteristics.

The move suppression coefficients in multivariable DMC follow a notation that differs from that of SISO DMC. Λ is a square-diagonal matrix with dimensions $M \cdot S \times M \cdot S$. This matrix can be divided into S^2 square blocks, each with dimensions $M \times M$. The leading diagonal elements of the first $M \times M$ matrix block along the diagonal of Λ are λ_1 , the leading diagonal elements of the next $M \times M$ matrix block along the diagonal of Λ are λ_2 , and so on. All of the off-diagonal elements of the matrix Λ are zero. Thus, in the multivariable DMC control law (eq 5), the move suppression coefficients that are added to the leading diagonal of the multivariable system matrix ($\mathbf{A}^T \mathbf{\Gamma}^T \mathbf{\Gamma} \mathbf{A}$) are λ_i^2 ($i = 1, 2, \dots, S$).

Building upon the analogy, an approximation of the multivariable DMC system matrix ($\mathbf{A}^T \mathbf{\Gamma}^T \mathbf{\Gamma} \mathbf{A}$) comprised of S^2 matrix blocks can be derived. The S^2 matrix blocks, each with dimensions $M \times M$, have a form identical to that obtained earlier (eq 33) from a similar approximation of the scaled single-loop DMC system matrix, $\tilde{\mathbf{A}}^T \tilde{\mathbf{A}}$. Note that only the processes that exhibit integrating behavior will have this form.

The impact of a change in the i th controller output on all measured process variables is reflected in the i th diagonal matrix block. Hence, it is possible to select the i th move suppression coefficient, λ_i^2 , such that the condition number of the i th diagonal matrix block is always bounded by a fixed low value. When the condition number of the i th diagonal matrix block is held at a low value, a desirable closed-loop performance is achieved while preventing the i th controller output move size from becoming excessive.

With this understanding, an analytical expression that computes the move suppression coefficients for

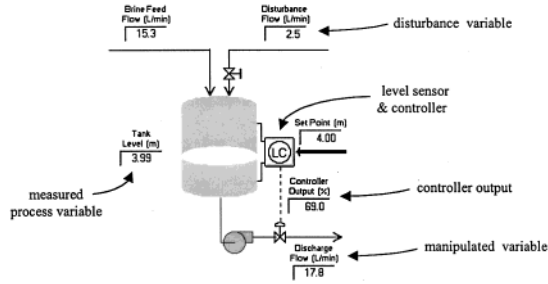


Figure 5. Pumped tank graphic from the Control Station software package.

multivariable DMC where some of the subprocesses exhibit integrating behavior can be obtained as

$$\lambda_i^2 = \frac{M}{10} \sum_{j=1}^R \left[\gamma_j^2 K_{ij}^2 \left(P - k_{ij} - \frac{3}{2} \frac{\tau_{p_{ij}}}{T} + 2 - \frac{(M-1)}{2} \right) \right] +$$

Sub-processes that do not exhibit integrating behavior

$$\frac{1}{10M} \sum_{j=1}^R \left[\gamma_j^2 K_{ij}^{*2} T^2 \left(\frac{M^2 (P - k_{ij} + 1)^3}{3} - 0.08 M^3 (P - k_{ij} + 1)^2 \right) \right]$$

Sub-processes that do exhibit integrating behavior

($i = 1, 2, \dots, S$) (45)

Using eq 45, the S move suppression coefficients, one for each controller output, can be computed for a given sampling time, T , control horizon, M , and controlled variable weights, γ_i . The tuning guidelines for MIMO DMC of integrating processes are summarized in Table 3.

5. Validation of the New Tuning Rules

5.1. Single-Loop Process. The pumped tank process, shown in Figure 5, is a liquid surge tank. This simulation is one of the case studies available in Control Station. The measured process variable is the liquid level. The controller manipulates the liquid flow rate out of the bottom of the tank by adjusting a throttling valve at the discharge of a constant-pressure pump to maintain the level in the tank. The disturbance variable is the flow rate of a secondary feed to the tank.

The height of the liquid in the tank does not impact the discharge flow rate; hence, this is an example of an integrating process. For example, when the total flow rate into the tank is greater than the discharge flow rate, the tank level will continue to rise until the tank is full, and when the total flow rate into the tank is less than the discharge flow rate, the tank level will fall until empty.

Following Table 2, the first step in tuning is to fit a FOPDT integrating model to process data. Here a FOPDT integrator model fit yields the parameters for the pumped tank process as $K_p^* = -0.02$ m/(%·min) and $\theta_p = 1.0$ min. Using eq 12, $T = 30$ s is calculated. For the FOPDT integrating parameters estimated and using the value of T above, the prediction horizon, P , and the model horizon, N , are computed using eq 16 to be 32, which equals the closed-loop settling time of the pumped tank process in samples. Next, a control horizon, M , of 8 is selected using eq 17. Finally, a move suppression coefficient of 0.7 is computed for the pump tank process using eq 44.

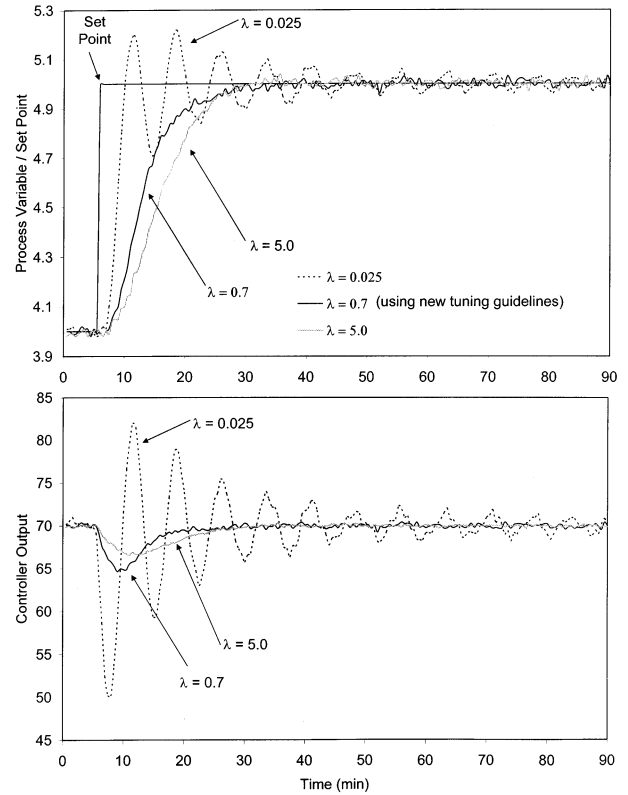


Figure 6. Effect of the move suppression coefficient for set-point tracking capabilities for the pumped tanks ($T = 30$, $P = N = 32$, and $M = 8$).

The control objective is the set-point tracking capabilities for the controller due to a step change in the set-point. A desirable closed-loop performance is defined as no peak overshoot and a fast rise time.

The significant impact of the move suppression coefficient on performance is illustrated in Figure 6. The move suppression calculated using the new tuning guidelines is 0.7. When the move suppression coefficient is reduced in magnitude, the controller output moves become increasingly aggressive, resulting in a process variable response that oscillates with a large overshoot. When the move suppression coefficient is decreased, the penalty on the move sizes made by DMC is reduced, resulting in more aggressive moves. When the move suppression coefficient is increased in magnitude, the response becomes sluggish with a longer rise time.

Although the previously published tuning guidelines^{5,6} are not shown in the figure, the calculated values based on fitting of a FOPDT model approximation and the tuning guidelines given in Table 1 are given below. A FOPDT model approximation of the process yields a $K_p = -2.3$ m/%, $\tau_p = 95.0$ min, and $\theta_p = 1.3$ min. The sample time is selected such that T is equal to 30 s, which is reasonable for the system being studied. Using the tuning guidelines given in Table 1, the prediction horizon and model horizon are calculated to be 956, the control horizon is found to be 193, and the value calculated for the move suppression coefficient is 5.64×10^4 . Because the FOPDT model approximation is not representative of the actual system being studied, the approximated model parameters give values for the horizons that are too long, which will increase the computational load, and a value for the move suppression coefficient that is too large. Hence, an undesirable closed-loop performance will be observed.

Table 3. Tuning Guidelines for MIMO DMC of Integrating (Non-Self-Regulating) Processes

1. approximate the process dynamics of controller output to measured process variable pairs of the integrating subprocesses with the FOPDT integrating model

$$\frac{y_j(s)}{u_i(s)} = \frac{K_{p_{ij}}^* e^{-\theta_{p_{ij}} s}}{s} \quad (i = 1, 2, \dots, S; j = 1, 2, \dots, R)$$

2. approximate the process dynamics of controller output to measured process variable pairs of nonintegrating subprocesses with the FOPDT model

$$\frac{y_j(s)}{u_i(s)} = \frac{K_{p_{ij}} e^{-\theta_{p_{ij}} s}}{\tau_{p_{ij}} s + 1} \quad (i = 1, 2, \dots, S; j = 1, 2, \dots, R)$$

3. select the sample time as close as possible to

$$T = \min \left[\underbrace{\max(0.1\tau_{p_{ij}}, \theta_{p_{ij}})}_{\text{for non-integrating sub-processes}}, \underbrace{0.5\theta_{p_{ij}}}_{\text{for integrating sub-processes}} \right] \quad (i = 1, 2, \dots, S; j = 1, 2, \dots, R)$$

4. approximate the closed-loop time constant of the integrating subprocesses

$$\tau_{CL_{ij}} = \theta_{p_{ij}} \sqrt{10} \quad (i = 1, 2, \dots, S; j = 1, 2, \dots, R)$$

5. compute the prediction horizon, P , and the model horizon, N

$$P = N = \max \left[\underbrace{\left(\frac{5\tau_{p_{ij}}}{T} + k_{ij} \right)}_{\text{for non-integrating sub-processes}}, \underbrace{\left(\frac{5\tau_{CL_{ij}}}{T} + k_{ij} \right)}_{\text{for integrating sub-processes}} \right] \quad \text{where } k_{ij} = \text{Int} \left(\frac{\theta_{p_{ij}}}{T} + 1 \right) \\ (i = 1, 2, \dots, S; j = 1, 2, \dots, R)$$

6. compute a control horizon, M

$$M = \max \left[\underbrace{\left(\frac{\tau_{p_{ij}}}{T} + k_{ij} \right)}_{\text{for non-integrating sub-processes}}, \underbrace{\left(\frac{\tau_{CL_{ij}}}{T} + k_{ij} \right)}_{\text{for integrating sub-processes}} \right] \quad (i = 1, 2, \dots, S; j = 1, 2, \dots, R)$$

7. select the controlled variable weights, γ_j^2

8. compute the move suppression coefficient, λ^2

$$\lambda_i^2 = \frac{M}{10} \sum_{j=1}^R \left[\underbrace{\gamma_j^2 K_{ij}^2 \left(P - k_{ij} - \frac{3\tau_{p_{ij}}}{2T} + 2 - \frac{(M-1)}{2} \right)}_{\text{Sub-processes that do not exhibit integrating behavior}} \right] + \\ \frac{1}{10M} \sum_{j=1}^R \left[\underbrace{\gamma_j^2 K_{ij}^{*2} T^2 \left(\frac{M^2 (P - k_{ij} + 1)^3}{3} - 0.08M^3 (P - k_{ij} + 1)^2 \right)}_{\text{Sub-processes that do exhibit integrating behavior}} \right] \quad (i = 1, 2, \dots, S)$$

9. implement DMC using the traditional step response matrix of the actual process and the initial values of the parameters computed in steps 1–8

Process constraints were included to illustrate that the tuning guidelines are still valid even though they were derived for the unconstrained control law. The constraints considered in this investigation include

$$4 \leq \hat{y} \leq 5 \quad (46a)$$

$$-0.5 \leq \Delta \bar{\mathbf{u}} \leq 0.5 \quad (46b)$$

$$0 \leq \bar{\mathbf{u}} \leq 100 \quad (46c)$$

The control objective is the set-point tracking capabilities for the controller due to a step change in the

set-point. A desirable closed-loop performance is defined as no peak overshoot and a fast rise time.

Figure 7 displays the effect of adding process constraints to the modified DMC algorithm and the tuning guidelines. Based on $K_p^* = -0.02$ m/(%·min) and $\theta_p = 1.0$ min, $T = 30$ s, $P = N = 32$, $M = 8$, and $\lambda = 0.7$. As shown by Figure 7, both the constrained DMC and unconstrained DMC exhibit similar performances. Hence, the inclusion of constraints has no impact on the performance of the modified DMC algorithm or the tuning guidelines.

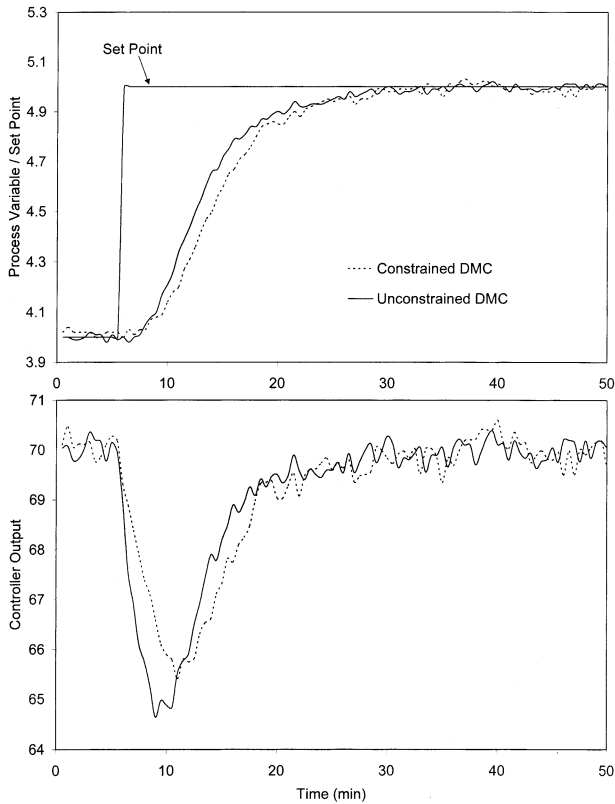


Figure 7. Effect of constraints for set-point tracking capabilities for the pumped tanks ($T = 30$, $P = N = 32$, $M = 8$, and $\lambda = 0.7$).

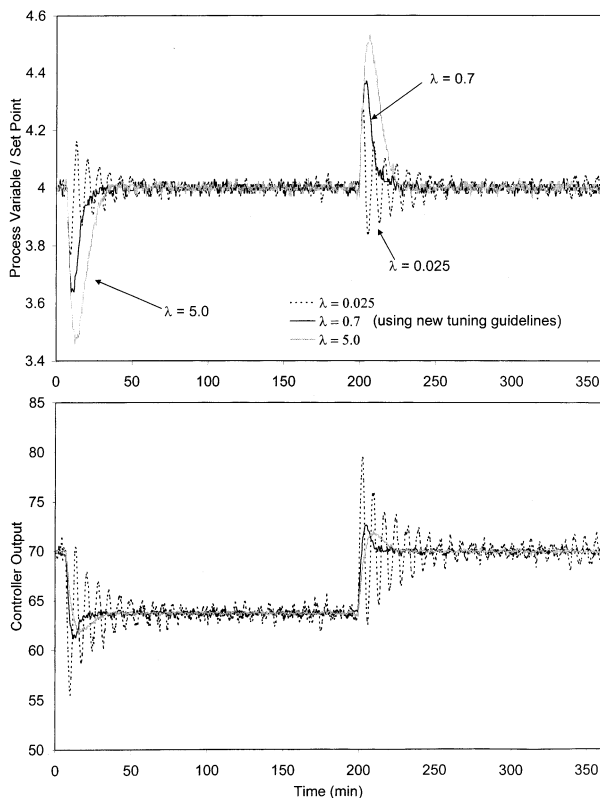


Figure 8. Effect of the move suppression coefficient for disturbance rejection for the pumped tanks ($T = 30$, $P = N = 32$, and $M = 8$).

The disturbance rejection capability of the DMC controller is also studied. The disturbance is the flow rate of a secondary feed to the tank. The disturbance

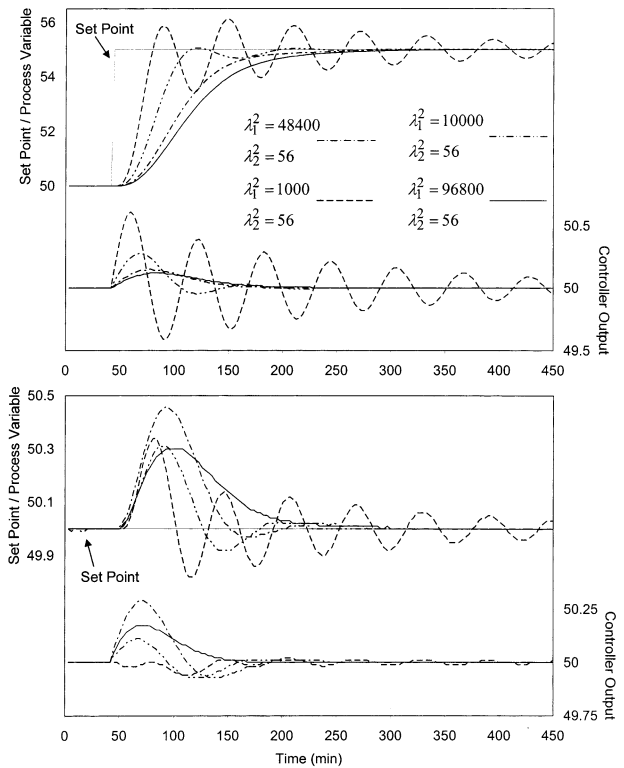


Figure 9. Effect of the move suppression coefficient for set-point tracking capabilities for the multivariable process ($T = 3$, $P = N = 50$, and $M = 14$).

flow rate is stepped from 2.5 to 1.0 mL/min and then back to 2.5 L/min.

Figure 8 shows the response of the process variables for the DMC implementation with three different move suppression coefficients. The control objective was to maintain the process variable at a set-point level of 4 m. The design goal was a small overshoot ratio and a quick settling time.

As shown by Figure 8, when $\lambda = 0.025$, the process variable oscillates and has a very long settling time. The value of the move suppression coefficient, $\lambda = 0.7$, calculated using eq 44, is also displayed on the graph. As shown, this controller has a shorter settling time but a slightly larger peak overshoot. When λ is increased to 5.0, the response of the process variable exhibits a large overshoot and a much slower settling time. Hence, this study shows that the proposed tuning strategy results in tuning parameters that effectively reject disturbances.

5.2. Multivariable Process. The tuning strategy, presented and validated in this paper for single-loop DMC, was extended to multivariable DMC as the analytical expression in eq 45. An example application of the tuning strategy extended to multivariable DMC, where one of the subprocesses exhibits integrating behavior, is demonstrated here for this system consisting of two controller outputs and two measured process variables. The system can be written as

$$\begin{bmatrix} y_1(s) \\ y_2(s) \end{bmatrix} = \begin{bmatrix} \frac{0.5e^{-2s}}{s(10.0s + 1)} & \frac{0.2 e^{-10s}}{15s + 1} \\ \frac{1.0e^{-10s}}{20.0s + 1} & \frac{1.5e^{-5s}}{15s + 1} \end{bmatrix} \begin{bmatrix} u_1(s) \\ u_2(s) \end{bmatrix} \quad (47)$$

All of the times are given in minutes.

As presented in Table 3, the first step in tuning is to fit a FOPDT integrating model to the subprocess in eq 47 exhibiting integrating behavior. Here the Design Tools module in Control Station yields the model parameters for the subprocess as $K_p^* = 0.5\%/(\%\cdot\text{min})$ and $\theta_p = 8.6$ min. A sample time, T , of 3.0 min was used in this study. The prediction horizon, P , and model horizon, N , were computed to include the steady-state terms in the step response of all manipulated variable and measured output pairs as

$$P = N = \max \left[\underbrace{\left(\frac{5\tau_{p_{ij}}}{T} + k_{ij} \right)}_{\text{for non-integrating sub-processes}}, \underbrace{\left(\frac{5\tau_{CL}}{T} + k_{ij} \right)}_{\text{for integrating sub-processes}} \right] \quad (i = 1, 2, \dots, S; j = 1, 2, \dots, R) \quad (48)$$

In this case, $P = N = 50$. The control horizon, M , was computed as

$$M = \max \left[\underbrace{\left(\frac{\tau_{p_{ij}}}{T} + k_{ij} \right)}_{\text{for non-integrating sub-processes}}, \underbrace{\left(\frac{\tau_{CL}}{T} + k_{ij} \right)}_{\text{for integrating sub-processes}} \right] \quad (i = 1, 2, \dots, S; j = 1, 2, \dots, R) \quad (49)$$

The control horizon, M , equals 14. Equal controlled variable weights were used for both measured outputs, i.e., $\Gamma^T \Gamma = \mathbf{I}$. The move suppression coefficients, $\Lambda^T \Lambda$, were computed from the analytical expression for multivariable DMC in eq 45. Equation 45 computes the diagonal elements of the matrix Λ as $\lambda_1^2 = 48\,400$ and $\lambda_2^2 = 56$.

The control objective in this study is set-point tracking of process variable 1 for a step change in the set-point from 50 to 55. The design goal is a quick rise time with no peak overshoot ratio and no oscillations.

Figure 9 illustrates the response of the two measured process variables and the corresponding controller output moves for a step change in the y_1 set-point. The move suppression coefficients calculated using the new tuning guidelines are $\lambda_1^2 = 48\,400$ and $\lambda_2^2 = 56$. The results in Figure 9 show that the analytical expression for multivariable DMC computes move suppression coefficients that result in a desirable closed-loop performance.

When the move suppression coefficients are reduced in magnitude to $\lambda_1^2 = 1000$ and $\lambda_2^2 = 56$, the controller output moves become increasingly aggressive, resulting in a process variable response that oscillates with a large overshoot. When the move suppression coefficient is decreased, the penalty on the move sizes made by DMC is reduced, resulting in more aggressive moves. When the move suppression coefficients are increased from $\lambda_1^2 = 1000$ and $\lambda_2^2 = 56$ to $\lambda_1^2 = 10\,000$ and $\lambda_2^2 = 56$, the response exhibits some oscillations with a smaller peak overshoot ratio. When the move suppression coefficient is increased in magnitude to values

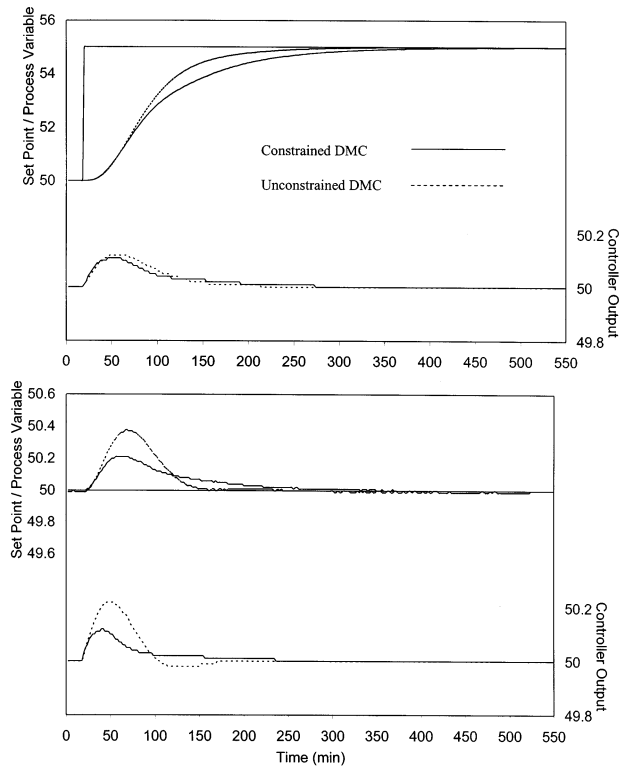


Figure 10. Effect of constraints for set-point tracking capabilities for the multivariable process ($T = 3$, $P = N = 50$, $M = 14$, $\lambda_1^2 = 48\,400$, and $\lambda_2^2 = 56$).

greater than those given by eq 45 ($\lambda_1^2 = 48\,400$ and $\lambda_2^2 = 56$), the response becomes sluggish with a longer rise time. This demonstration confirms that the tuning strategy presented for single-loop DMC holds potential for a formal extension to the more challenging problem of tuning multivariable DMC when some of the subprocesses exhibit integrating behavior.

Depending on the criterion for a good closed-loop performance for a given application, the condition number can be conveniently fixed. The choice of a condition number of 10 was motivated based on past research^{5,6} and a more conservative closed-loop response. However, if a faster or slower closed-loop response is more desirable, a larger or smaller condition number, respectively, can be used instead. In addition, a small closed-loop time constant corresponds to a faster closed-loop response with large variations in the controller output while a large closed-loop time constant displays a slower and smoother response.

Process constraints were included to illustrate that the tuning guidelines are still valid even though they were derived for the unconstrained control law. The constraints considered in this investigation include

$$45 \leq \hat{y}_1 \leq 55 \quad (50a)$$

$$-0.1 \leq \Delta \bar{\mathbf{u}}_1 \leq 0.1 \quad (50b)$$

$$0 \leq \bar{\mathbf{u}}_1 \leq 100 \quad (50c)$$

$$49 \leq \hat{y}_2 \leq 51 \quad (50d)$$

$$-0.1 \leq \Delta \bar{\mathbf{u}}_2 \leq 0.1 \quad (50e)$$

$$0 \leq \bar{\mathbf{u}}_2 \leq 100 \quad (50f)$$

Figure 10 displays the effect of adding process constraints to the modified DMC algorithm and the tuning

guidelines. Again, $T = 3$ min, $P = N = 50$, and $M = 14$. Equal controlled variable weights were used for both measured outputs, i.e., $\Gamma^T \Gamma = \mathbf{I}$. The move suppression coefficients, $\Lambda^T \Lambda$, were computed from the analytical expression for multivariable DMC in eq 45 as $\lambda_1^2 = 48\,400$ and $\lambda_2^2 = 56$.

As shown by Figure 10, both the constrained DMC and unconstrained DMC exhibit similar performances. In this case, unconstrained DMC exhibits a slightly better performance than constrained DMC, which is what would be expected. Hence, the inclusion of constraints does not have a negative impact on the performance of the modified DMC algorithm or the tuning guidelines.

6. Conclusions

A tuning strategy for multivariable DMC where the processes exhibit integrating behaviors, with a novel analytical expression for the move suppression coefficient, λ , was presented. The application of this tuning strategy was demonstrated through simulation studies. The DMC controller tuned using the above design strategy exhibited a good set-point tracking capability with no peak overshoot and a fast rise time. The disturbance rejection performance of DMC tuned with the proposed tuning strategy was also explored. The DMC controller tuned using the proposed design strategy effectively rejected disturbances that impacted the process.

Nomenclature

a_i = i th unit step response coefficient in SISO DMC
 \tilde{a}_i = i th gain- and time-scaled unit step response coefficient in SISO DMC
 \mathbf{A} = complete dynamic matrix in SISO and MIMO DMC
 $\tilde{\mathbf{A}}$ = gain- and time-scaled dynamic matrix in SISO DMC
 $\mathbf{A}^T \mathbf{A}$ = system matrix in SISO DMC
 $\mathbf{A}^T \mathbf{A} + \lambda \mathbf{I}$ = overall system matrix in SISO DMC
 $\tilde{\mathbf{A}}^T \tilde{\mathbf{A}}$ = gain- and time-scaled system matrix in SISO DMC
 $\tilde{\mathbf{A}}^T \tilde{\mathbf{A}} + f \mathbf{I}$ = gain- and time-scaled overall system matrix in SISO DMC
 $\mathbf{A}^T \Gamma^T \Gamma \mathbf{A}$ = system matrix in MIMO DMC
 $\mathbf{A}^T \Gamma^T \Gamma \mathbf{A} + \Lambda^T \Lambda$ = overall system matrix in MIMO DMC
 c = condition number of the overall system matrix in SISO and MIMO DMC
 c_j = i th term of the pseudo inverse matrix in SISO DMC
 \tilde{c}_i = i th term of the gain- and time-scaled pseudo inverse matrix in SISO DMC
 d = prediction error in SISO DMC
 $\tilde{\mathbf{e}}$ = vector of predicted errors for the process variable in SISO DMC and for all R process variables in MIMO DMC
 f = gain- and time-scaled move suppression coefficient in SISO DMC
 $G_p(s)$ = continuous process transfer function
 $G(z)$ = discrete process transfer function
 $\tilde{G}(z)$ = gain- and time-scaled discrete process transfer function
 i = index
 \mathbf{I} = identity matrix
 j = index for sampling instants
 J = DMC performance objective
 k = discrete dead time in a SISO system
 k_{rs} = discrete dead time of the subprocess relating the r th process variable and the s th controller output in a MIMO system
 K_p = self-regulating process gain
 K_p^* = non-self-regulating process gain

M = control horizon (number of controller output moves)
 n = current sampling instant
 N = model horizon (process settling time in samples)
 P = prediction horizon
 r = process variable index
 R = number of process variables
 s = controller output index
 (s) = Laplace domain operator
 S = number of controller outputs in a MIMO system
 t = continuous time
 T = sample time
 T_{rs} = sample time relating the r th process variable and s th controller output in a MIMO system
 u_s = s th controller output
 y_r = r th process variable
 y_0 = initial condition of the process variable in a SISO system
 $\hat{y}(n+j)$ = predicted process variable j sample times into the future in a SISO system
 z = discrete time shift operator

Greek Symbols

$\tilde{\alpha}_{ij}$ = term in the i th row and j th column of the DMC system matrix
 β = constant difference in $\tilde{\mathbf{A}}^T \tilde{\mathbf{A}}$ row-wise terms from left to right
 $\Delta \tilde{\mathbf{u}}$ = vector of computed moves for all S controller output variables
 Δu_i = controller output move [= $u(i) - u(i-1)$] at the i th sampling instant
 γ_r^2 = r th controlled variable weight in MIMO DMC
 λ = move suppression coefficient in SISO DMC
 λ_s^2 = s th move suppression coefficient in MIMO DMC
 $\Gamma^T \Gamma$ = matrix of controlled variable weights, γ_r^2 , in MIMO DMC
 $\Lambda^T \Lambda$ = matrix of move suppression coefficients, λ_s^2 , in MIMO DMC
 θ_p = effective dead time
 μ = eigenvalue
 μ_{\min} = minimum absolute eigenvalue of the approximate $\tilde{\mathbf{A}}^T \tilde{\mathbf{A}}$ matrix in SISO DMC
 μ_{\max} = maximum absolute eigenvalue of the approximate $\tilde{\mathbf{A}}^T \tilde{\mathbf{A}}$ matrix in SISO DMC
 τ_{CL} = overall closed-loop time constant
 τ_p = overall process time constant

Abbreviations

DMC = dynamic matrix control
 FOPDT = first-order plus dead time
 MIMO = multiple-input multiple-output
 MPC = model predictive control
 PI = proportional integral
 PID = proportional integral derivative
 SISO = single-input single-output
 QDMC = quadratic dynamic matrix control

Literature Cited

- (1) Cutler, C. R.; Ramaker, D. L. Dynamic Matrix Control-A Computer Control Algorithm. Proceedings of JACC, San Francisco, CA, 1980.
- (2) Marchetti, J. L.; Mellichamp, D. A.; Seborg, D. E. Predictive Control Based on Discrete Convolution Models. *Ind. Eng. Chem. Process Des. Dev.* **1983**, *22*, 488.
- (3) Ogunnaike, B. A. Dynamic Matrix Control: A Nonstochastic, Industrial Process Control Technique with Parallels in Applied Statistics. *Ind. Eng. Chem. Fundam.* **1986**, *25*, 712.
- (4) Garcia, C. E.; Morshedi, A. M. Quadratic Programming Solution of Dynamic Matrix Control (QDMC). *Chem. Eng. Commun.* **1986**, *46*, 73.

- (5) Shridhar, R.; Cooper, D. J. A Tuning Strategy for Unconstrained SISO Model Predictive Control. *Ind. Eng. Chem. Res.* **1997**, *36*, 729.
- (6) Shridhar, R.; Cooper, D. J. A Tuning Strategy for Unconstrained Multivariable Model Predictive Control. *Ind. Eng. Chem. Res.* **1998**, *37*, 4003.
- (7) Lundström, P.; Lee, J. H.; Morari, M.; Skogestad, S. Limitations of Dynamic Matrix Control. *Comput. Chem. Eng.* **1995**, *19* (4), 409.
- (8) Lee, J.; Morari, H. M.; García, C. E. State-space interpretation of model predictive control. *Automatica* **1994**, *30*, 707–717.
- (9) Gupta, Y. P. Control of Integrating Processes Using Dynamic Matrix Control. *Trans. Inst. Chem. Eng.* **1998**, *76A*, 465.
- (10) Chien, I. L.; Fruehauf, P. S. Consider IMC Tuning to Improve Controller Performance. *Chem. Eng. Prog.* **1990**, Oct, 33–41.
- (11) Tyreus, B. D.; Luyben, W. L. Tuning PI Controllers for Integrator/Dead Time Processes. *Ind. Eng. Chem. Res.* **1992**, *31*, 2625–2628.
- (12) Seborg, D. E.; Edgar, T. F.; Mellichamp, D. A. *Process Dynamics and Control*; John Wiley & Sons: New York, 1989.
- (13) Franklin, G. F.; Powell, J. D. *Digital Control of Dynamic Systems*; Addison-Wesley Publishing Co.: Reading, MA, 1980.
- (14) Åström, K. J.; Wittenmark, B. In *Computer Controlled Systems, Theory and Design*; Kailath, T., Ed.; Information and System Science Series; Prentice Hall: Englewood Cliffs, NJ, 1984.
- (15) Prett, D. M.; García, C. E. *Fundamental Process Control*; Butterworth: Boston, MA 1988.
- (16) Maurath, P. R.; Mellichamp, D. A.; Seborg, D. E. Predictive Controller Design for Single Input/Single Output Systems. *Ind. Eng. Chem. Res.* **1988**, *27*, 956.
- (17) Gupta, Y. P. *A Simplified Model Predictive Control Approach*; Department of Chemical Engineering, TUNS: Halifax, Canada, 1987.
- (18) Gupta, Y. P. Characteristic Equations and Robust Stability of a Simplified Predictive Control Algorithm. *Can. J. Chem. Eng.* **1993**, *71*, 617.
- (19) Hoerl, A. E.; Kennard, R. W. Ridge Regression: Biased Estimation for Nonorthogonal Problems. *Technometrics* **1970**, *12* (1), 55.

Received for review July 22, 2002

Revised manuscript received January 29, 2003

Accepted February 13, 2003

IE020546P